ORIGINAL RESEARCH

Aortic Valve Stenosis Alters Expression of Regional Aortic Wall Shear Stress: New Insights From a 4-Dimensional Flow Magnetic Resonance Imaging Study of 571 Subjects

Pim van Ooij, PhD; Michael Markl, PhD; Jeremy D. Collins, MD; James C. Carr, MD; Cynthia Rigsby, MD; Robert O. Bonow, MD; S. Chris Malaisrie, MD; Patrick M. McCarthy, MD; Paul W.M. Fedak, MD, PhD; Alex J. Barker, PhD

***Background*—**Wall shear stress (WSS) is a stimulus for vessel wall remodeling. Differences in ascending aorta (AAo) hemodynamics have been reported between bicuspid aortic valve (BAV) and tricuspid aortic valve patients with aortic dilatation, but the confounding impact of aortic valve stenosis (AS) is unknown.

***Methods and Results*—**Five hundred seventy-one subjects underwent 4-dimensional flow magnetic resonance imaging in the thoracic aorta (210 right-left BAV cusp fusions, 60 right-noncoronary BAV cusp fusions, 245 tricuspid aortic valve patients with aortic dilatation, and 56 healthy controls). There were 166 of 515 (32%) patients with AS. WSS atlases were created to quantify group-specific WSS patterns in the AAo as a function of AS severity. In BAV patients without AS, the different cusp fusion phenotypes resulted in distinct differences in eccentric WSS elevation: right-left BAV patients exhibited increased WSS by 9% to 34% ($P<0.001$) at the aortic root and along the entire outer curvature of the AAo whereas right-noncoronary BAV patients showed 30% WSS increase ($P<0.001$) at the distal portion of the AAo. WSS in tricuspid aortic valve patients with aortic dilatation patients with no AS was significantly reduced by 21% to 33% ($P<0.01$) in 4 of 6 AAo regions. In all patient groups, mild, moderate, and severe AS resulted in a marked increase in regional WSS ($P<0.001$). Moderate-to-severe AS further increased WSS magnitude and variability in the AAo. Differences between valve phenotypes were no longer apparent.

***Conclusions*—**AS significantly alters aortic hemodynamics and WSS independent of aortic valve phenotype and over-rides previously described flow patterns associated with BAV and tricuspid aortic valve with aortic dilatation. Severity of AS must be considered when investigating valve-mediated aortopathy. **(*J Am Heart Assoc*. 2017;6:e005959. DOI: 10.1161/JAHA.117.005959.)**

Key Words: aortic disease • aortic valve • aortic valve stenosis • bicuspid aortic valve • magnetic resonance imaging

Ascending aortic aneurysms are life threatening because of the increased risk for aortic dissection and rupture. Evidence strongly implicates genetic mechanisms for selected aortic diseases such as Marfan syndrome, but the underlying cause of ascending aortic aneurysm formation in other aortic diseases is less well understood.[1,2] For example, many patients with congenital bicuspid aortic valve (BAV) develop ascending aortic dilatation,[3,4] in whom the underlying causative mechanisms are not clear.[5] Genetic variants may contribute to BAV mediated aortopathy, but no common or unifying genetic pattern has emerged. The consistent observation of BAV-mediated alterations in ascending aortic blood flow patterns, even without clinically relevant valve dysfunction,[6,7] has formed the basis for a hemodynamic hypothesis which postulates that regional BAV aortopathy is attributed to the impact of these altered blood flow patterns on vessel wall remodeling.[2,8,9]

Given that a large proportion of BAV subjects can also develop aortic stenosis (AS), a known independent risk factor for ascending aneurysm formation, studies investigating BAV-mediated aortopathy are often confounded. In other patient groups, such as those with trileaflet aortic valves and thoracic aortic dilatation (TAV-TAA), abnormal blood flow is also known to be present, both with and without AS.[10,11]

From the Department of Radiology, Academic Medical Center, Amsterdam, The Netherlands (P.v.O.); Departments of Radiology (P.v.O., M.M., J.D.C., J.C.C., A.J.B.) and Medicine–Cardiology (R.O.B.), and Division of Surgery-Cardiac Surgery (S.C.M., P.M.M., P.W.M.F.), Northwestern University Feinberg School of Medicine, Chicago, IL; Department of Biomedical Engineering, Northwestern University, Chicago, IL (M.M.); Department of Medical Imaging, Ann & Robert H Lurie Children's Hospital of Chicago, IL (C.R.); Department of Cardiac Sciences, University of Calgary, Calgary, Alberta, Canada (P.W.M.F.).

Correspondence to: Alex J. Barker, PhD, Department of Radiology, Northwestern University Feinberg School of Medicine, 737 N Michigan Ave, Suite 1600, Chicago, IL 60611. E-mail: alex.barker@northwestern.edu

Received April 3, 2017; accepted July 12, 2017.

Clinical Perspective

What Is New?

- This cross-sectional study is the largest 4-dimensional flow magnetic resonance imaging study to investigate the bicuspid aortic valve and distinct patterns of expression for blood wall shear stress on the ascending aorta wall, as stratified by aortic valve phenotype and stenosis severity.
- Distinct "wall shear stress" patterns exist for bicuspid aortic valve patients without aortic valve stenosis; however, bicuspid patients with significant stenosis exhibit very similar patterns to tricuspid aortic valve patients with stenosis.

What Are the Clinical Implications?

- The data provide an explanation for growing evidence that aortopathy in patients with a bicuspid aortic valve and valvular stenosis is not unique and very similar to the degree of aortopathy in those with tricuspid aortic valve and valvular stenosis.

Studies have confirmed that the modified hemodynamic environment associated with aortic dilatation and valve abnormalities will cause altered wall shear stress (WSS), a known mechanotransduction stimulus impacting cell function and influencing aortic wall remodeling.[12,13] Furthermore, advances in imaging have enabled the robust use of 4-dimensional (4D) flow magnetic resonance imaging (MRI), a technique which is capable of measuring 3-dimensional (3D) blood velocity and WSS in the entire volume of the thoracic aorta.[14] For example, a recent 4D flow MRI study in BAV patients demonstrated strong relationships between elevated aortic WSS and locations of regional aortopathy, as determined by aortic wall tissue histopathology (protein expression and tissue architecture).[8] Based on these data, and the hypothesis that altered aortic WSS is a potential physiological mechanism contributing to the risk for development of aortopathy, further understanding regarding the impact of aortic valve phenotype and AS severity on 3D WSS is needed. This includes coverage of the WSS measurement over the entire surface of the ascending aorta. Therefore, in this study, we use a large cohort of subjects to comprehensively investigate whether: (1) BAV cusp fusion morphology is associated with distinct patterns of expression of regionally elevated 3D WSS in the aorta as compared with TAV patients and (2) acquired valvular AS significantly alters aortic hemodynamics and 3D WSS beyond the effects of congenital aortic valve morphology. The findings from this work will provide novel information regarding the impact of AS on the distribution of 3D WSS in the ascending aorta (AAo) in the presence of TAV and BAV.

Methods

Study Design

An institutional 4D flow MRI database consisting of 804 postprocessed baseline exams was queried for adult patients under surveillance for aortic dilatation and/or aortic valve disease between November 2011 and January 2014. The objective was to identify BAV patients with clearly defined aortic valve morphology and to match a cohort of TAV patients with suspected aortopathy, as identified by an AAo greater than 4 cm in diameter. For AS and aortic regurgitation, all degrees of severity (or lack thereof) were considered for inclusion. For the BAV and TAV groups, past aortic or aortic valve surgery (n=65) or undetermined valve morphology (n=49) were exclusionary. Among the remaining patients with BAV, n=17 were further excluded because of nondiagnostic images, and n=11 were excluded because of diagnosis of unicuspid, functionally unicuspid (Sievers Type 2) or quadricuspid aortic valves. Among the remaining patients with TAV, n=136 were excluded because of the lack of evidence for aortopathy (ie, no AAo dilation greater than 4 cm in diameter) and n=11 were excluded because of nondiagnostic images. Thus, 515 MRI patient exams remained for analysis. In order to establish normal physiological WSS values, a control cohort consisting of 56 healthy volunteers with no history of cardiovascular disease and a normal functional TAV were enrolled. Informed consent was obtained from all controls. All patients undergoing standard-of-care MRI were enrolled by retrospective chart review and waiver of consent. All subjects were included in the study according to procedures approved by the Northwestern University Institutional Review Board.

Study Cohort

Of the 515 patient MRI exams, 270 patients had BAV (196 men; median age, 49 years; interquartile range [IQR], 37–59) and 245 patients had a TAV with aortic dilatation (subsequently referred to as TAV-TAA; 196 men; median age, 61 years; IQR: 52–70). The 56 healthy control subjects (38 men; median age, 45 years; IQR, 32–52) had a normally functioning and conventional TAV with no known cardiovascular disease.

Magnetic Resonance Imaging

MRI was performed on 1.5 or 3 Tesla MRI systems (Avanto, Espree, Aera, Skyra; Siemens Medical Systems, Erlangen, Germany). All subjects underwent a standard-of-care thoracic cardiovascular MRI exam including 2-dimensional (2D) time-resolved ECG gated (CINE) balanced steady state free precession imaging of the heart and aortic valve as well as 3D

contrast-enhanced magnetic resonance angiography following the administration of contrast media (either 0.2 mmol/kg of gadopentate dimeglumine, 0.1 mmol/kg of gadobenate dimeglumine, or 0.1 mmol/kg of gadofosveset trisodium) to provide a comprehensive evaluation of aortic morphology and valve function as previously reported.[15,16] In addition, 4D flow MRI (time-resolved 3-directional phase contrast MRI with 3D velocity encoding) was acquired in a sagittal oblique 3D volume covering the thoracic aorta using prospective ECG gating and a respiratory navigator gating.[17] 4D flow pulse sequence parameters were as follows: spatial resolution=2.2 to 4.2 mm×1.7 to 2.9 mm×2.2 to 4.0 mm; field of view=320 to 470 mm×234 to 382 mm×66 to 120 mm; temporal resolution=32.8 to 43.2 ms (11–31 cardiac time frames); echo time=2.1 to 2.8 ms; repetition time=4.1 to 5.4 ms; flip angle=7 to 15°. Velocity encoding sensitivity (venc) was adjusted to minimize velocity aliasing (venc=150–450 cm/s) based on 2D phase contrast MRI scout images.

Assessment of Aortic Valve Morphology and Aortic Dimensions

2D CINE steady state free precession data at the level of the aortic valve was used to confirm trileaflet valve morphology and to assess BAV fusion patterns. BAV cusp fusion patterns were categorized according to the scheme proposed by Sievers and Schmidtke[18] by an experienced radiologist. Patients with Sievers BAV type 0 AP and Sievers BAV type 1 L-R were combined into a group with valves opening in the anterior-posterior direction (fusion of the right- and left-coronary valve cusps, "RL-BAV"). Patients with BAV Sievers Type 0 LAT and Sievers type 1 R-N were combined into a group with valves opening in the lateral direction (fusion of the right- and noncoronary valve cusps, "RN-BAV"). To assess aorta caliber, contrast-enhanced magnetic resonance angiography images were analyzed using a multiplanar reformat by experienced radiologists to measure the diameter of the aorta in the cross-sectional view, according to practice guidelines.[19] Diameters at the sinuses of Valsalva and mid-ascending aorta were recorded.

4D Flow Data Analysis

All 4D flow MRI data were corrected for eddy currents, Maxwell terms, and velocity aliasing using custom built software programmed in Matlab (The MathWorks, Inc, Natick, MA).[20] 3D phase contrast MR angiograms were computed based on the 4D flow data and used to obtain a 3D segmentation of the aorta using a commercial software package (Mimics; Materialise, Leuven, Belgium).[21] To quantify degree of AS in patients, peak velocity during systole was quantified at the aortic root using an oblique sagittal maximum intensity projection of the absolute velocity.[22] Degree of AS was classified according to current guidelines with respect to the peak transvalvular vena contracta velocity, that is, no AS: <2.0 m/s; mild AS: 2.0 to 2.9 m/s; moderate AS: 3.0 to 3.9 m/s; and severe AS: ≥4.0 m/s.[23] To simplify data interpretation, 3 AS groups were created, defined as patients having no AS, those with mild AS, and those with moderate and severe AS. Aortic regurgitation was assessed according MRI recommendations.[24] Based on the 3D segmentation, systolic 3D WSS along the entire aortic wall was calculated from 4D flow velocity data using a previously described algorithm.[25] Briefly, the WSS vector was estimated at the wall based on the 3D spatial velocity gradient perpendicular to the vessel wall. Systolic 3D WSS magnitude along the entire aorta surface was then calculated at peak systole.[14]

3D WSS Atlas

A previously described "atlas" concept was used to spatially register aortic geometries across a large number of subjects.[12] This approach allows for the calculation of a cohort-averaged systolic 3D WSS map to be displayed on a group-specific aorta surface (hereafter solely referred to as a "WSS atlas"). The data analysis workflow to generate a WSS atlas for a specific patient cohort is illustrated in Figure 1. WSS atlases were created for the following cohorts: normal controls, RL-BAV patients, RN-BAV patients, and TAV-TAA patients. The 3 patient cohorts (RL-BAV, RN-BAV, and TAV-TAA) were further stratified by those with none, mild, and moderate-to-severe AS. For each cohort, a "shared aorta geometry" was created by a previously described rigid registration approach, which maximizes the overlap of all aortic segmentations in the group.[12] Next, the systolic 3D WSS data were calculated for each individual patient and then interpolated to the group-specific shared aorta geometry. The systolic 3D WSS atlas was then generated by calculating the median and IQR of the WSS over all subjects in each group. The resulting WSS (mapped onto the shared aorta geometry) illustrates the spatial distribution of the cohort-averaged WSS on the 3D shared geometry (representing a cohort-specific WSS atlas). For quantification of patient-specific regional WSS after registration to the shared geometry, the WSS atlas was subdivided into 6 regions at: (1) the inner AAo root; (2) the outer AAo root; (3) the inner proximal AAo; (4) the outer proximal AAo; (5) the inner distal AAo; and (6) the outer distal AAo (Figure 1, right).

Statistical Analysis

All continuous variables are reported as median and IQR. To compare parameters for subject demographics among groups, a Kruskal–Wallis 1-way ANOVA (for non-Gaussian distributions) was used. A Fisher exact test was used to compare categorical variables across groups. An ANCOVA of

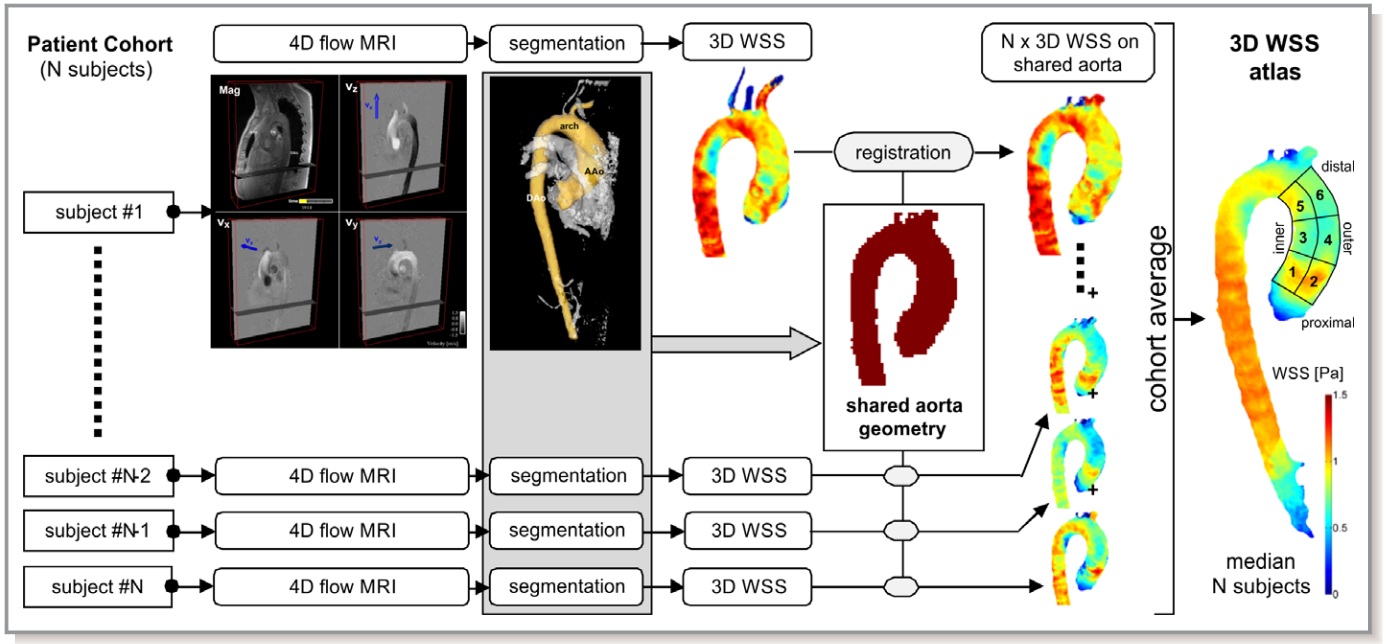

Figure 1. Data analysis workflow for the calculation of a cohort specific 3D wall shear stress (WSS) atlas. WSS quantification was performed in the numbered regions of interest: (1) the inner sinotubular junction, (2) the outer sinotubular junction, (3) the inner proximal ascending aorta (AAo), (4) the outer proximal AAo, (5) the inner distal AAo, and (6) the outer distal AAo. 3D indicates 3-dimensional; 4D, 4-dimensional; MRI, magnetic resonance imaging.

the ranks of WSS with age and sex as covariates was performed to assess WSS between groups. If the parameter was significantly different between groups ($P<0.05$ with Bonferroni correction), multiple comparisons for all groups were performed using a *t* test on the WSS ranks. For all pair-wise comparisons, Bonferroni correction was used to adjust for multiple comparisons. Three main comparisons were performed to investigate the role of dilatation, valve morphology, and valve stenosis: (1) aortopathy and valve morphology without stenosis: controls versus TAV-TAA versus RL-BAV versus RN-BAV without stenosis; (2) aortopathy and valve morphology with mild stenosis: controls versus TAV-TAA versus RL-BAV versus RN-BAV with mild stenosis; and (3) aortopathy and valve morphology with moderate and severe stenosis: controls versus TAV-TAA versus RL-BAV versus RN-BAV with moderate and severe stenosis.

Results

Study Cohort

The demographics of the study cohort are summarized in Table 1 (note: the method in Garcia et al was used to measure the mid-ascending aorta [MAA] in the control population).[26] Of the 515 patients, 88 (17%) had mild AS: 19 with TAV-TAA (8% of all TAV-TAA); 54 with RL-BAV (26% of all RL-BAV); and 15 with RN-BAV (25% of all RN-BAV). There were 78 (15%) patients with moderate or severe AS: 13 (5%) with TAV-TAA; 43 (20%) with RL-BAV; and 22 (37%) with RN-BAV. For those with no and mild AS, subjects with TAV-TAA were significantly older ($P<0.001$). For patients with TAV-TAA without AS, the diameter at the level of the sinuses of Valsalva was larger ($P<0.001$) compared with the BAV groups.

Figure 2 shows representative examples of 4D flow-derived systolic 3D blood flow velocities in the thoracic aorta side by side with the patients' aortic valve morphology and left ventricular outflow. For subjects without AS (Figure 2, left column), aortic valve images revealed normal valve opening at peak systole for all subjects in all 4 cohorts (controls, TAV-TAA, RL-BAV, and RN-BAV) and congenitally altered valve morphology for RL-BAV and RN-BAV. BAV patients without stenosis exhibited eccentric outflow jets in the AAo (Figure 2D and 2F, red color and black arrow), which were absent in the control subjects and patients with TAV-TAA (Figure 2A and 2B). In addition, different BAV cusp fusion types (RL-BAV versus RN-BAV) resulted in different outflow jet orientations, indicating an association of BAV morphology with altered aortic hemodynamics. In contrast, patients with moderate or severe AS (Figure 2, right column) demonstrated impaired valve opening and more-pronounced high-velocity outflow jets in the AAo for all cohorts irrespective of valve type. Note that for the remainder of this article, the use of the term eccentric flow refers to a skewed flow profile, which produces nonuniform WSS values around the circumference of the vessel.

Table 1. Subject Demographics and Aortic Dimensions

All Subjects	Controls	TAV-TAA	RL-BAV	RN-BAV	*P* Value
N	56	245	210	60	…
% female	32	20	25	35	0.06
Age (y), median (IQR)	45 (32–52)	61 (52–70)*	50 (37–59)†	47 (40–58)†	<0.001
No AS					
N	56	213	113	23	…
% female	32	22§	24§	52	0.01
Age (y), median (IQR)	45 (32–52)	59 (49–69)*	40 (33–52)†	39 (33–44)†	<0.001
SOV (cm), median (IQR)	…‖	4.3 (4.0–4.6)	4.0 (3.6–4.4)†	3.9 (3.4–4.1)†	<0.001
MAA (cm), median (IQR)	3.2 (3.0–3.6)¶	4.0 (3.5–4.4)*	3.7 (3.2–4.3)*†	3.7 (3.1–4.4)*	<0.001
% with aortic dilatation#	0	100	42	18	…
Aortic insufficiency					
None (trace)/mild/moderate/severe/unavailable	…	127/64/19/1/2	52/41/9/3/8	12/9/0/0/2	
Mild AS					
N	…	19	54	15	…
% female	…	16	24	27	0.77
Age (y), median (IQR)	…	67 (62–73)	52 (46–62)†	49 (42–58)†	<0.001
SOV (cm), median (IQR)	…	3.9 (3.6–4.0)	4.1 (3.6–4.5)	4.1 (3.6–4.3)	0.47
MAA (cm), median (IQR)	…	4.3 (4.0–4.5)	4.2 (3.8–4.6)	4.0 (3.5–4.4)	0.50
% with aortic dilatation#	…	100	24	20	…
Aortic insufficiency					
None (trace)/mild/moderate/severe/unavailable		9/7/2/1/0	18/16/14/2/4	6/7/1/1/0	
Moderate and severe AS					
N	…	13	43	22	…
% female	…	8	30	23	0.24
Age (y), median (IQR)	…	67 (62–73)	61 (52–65)	58 (46–67)	0.06
SOV (cm), median (IQR)	…	4.0 (3.6–4.4)	3.8 (3.5–4.1)	4.0 (3.8–4.2)	0.10
MAA (cm), median (IQR)	…	4.2 (3.9–4.4)	3.9 (3.4–4.4)	4.1 (3.7–4.6)	0.12
% with aortic dilatation#	…	100	37	14	…
Aortic insufficiency					
None (trace)/mild/moderate/severe/unavailable		2/6/4/0/1	20/16/4/1/2	13/6/3/0/0	

AS indicates aortic stenosis; IQR, interquartile range; MAA, mid-ascending aorta; RL-BAV, right and left coronary leaflet fusion BAV; RN-BAV, right and noncoronary leaflet fusion BAV; SOV, sinuses of Valslava; TAV-TAA, tricuspid aortic valve with aortic dilation.

*Significantly different vs controls.

†Significantly different vs TAV-TAA.

‡Significantly different vs RL-BAV (note: no significances found for all subjects).

§Significantly different vs RN-BAV (Fisher exact test with Bonferroni correction).

‖No CE-MRA available, SOV diameter inaccurate with the method described by Garcia et al.[26]

¶No CE-MRA available, MAA diameter accurate with the method described by Garcia et al.[26]

#Defined as either SOV or MAA diameter >4 cm.

3D WSS Atlas

Registration of aortic 3D WSS to patient-specific shared aortic geometries for all patient cohorts (RL-BAV, RN-BAV, TAV-TAA, and controls) and AS severity groups (no AS, mild AS, severe, and moderate AS) resulted in the 10 unique 3D WSS atlases shown in Figure 3.

3D WSS in Patients With No AS

Compared with controls, patients with TAV-TAA showed significantly reduced WSS by 21% to 33% ($P<0.01$) in 4 aortic regions excepting those regions on the outer root and proximal AAo (Figure 3B; Table 2). Different BAV cusp fusion patterns (RL-BAV versus RN-BAV) resulted in distinct

differences in 3D WSS patterns: For RL-BAV patients, WSS was significantly elevated at the aortic root along the entire outer curvature of the AAo compared with controls and TAV-TAA (WSS was increased by 9% to 34% at the root, proximal AAo, and distal outer AAo; $P<0.001$). In contrast, RN-BAV patients presented with a more-localized WSS elevation at the

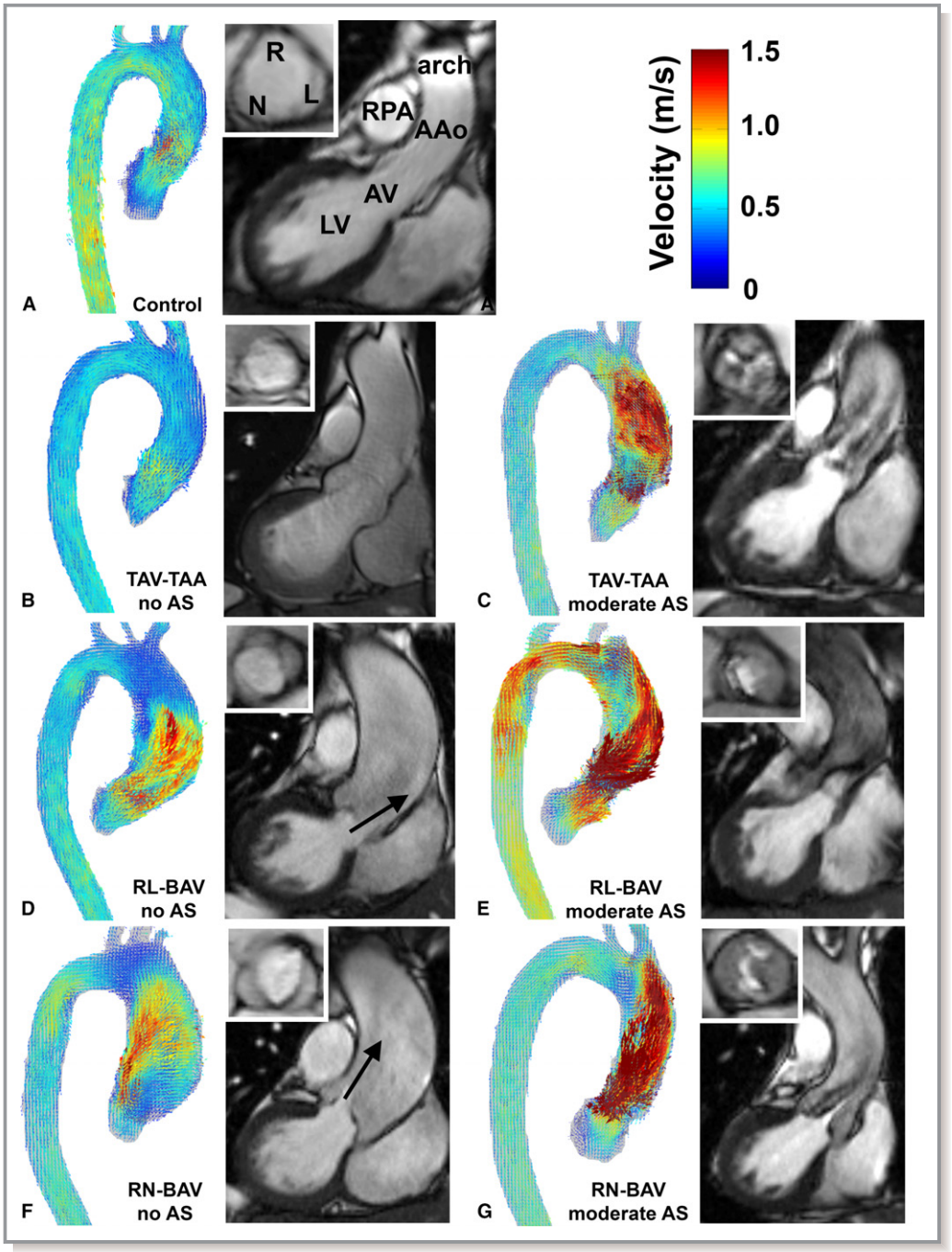

Figure 2. Representative examples of systolic 3D velocity fields in the aorta obtained by 4D flow MRI, aortic valve morphology (white inset box) and left ventricular outflow based on 2D CINE SSFP MRI for (A) controls, (B) TAV-TAA without AS, (C) TAV-TAA with moderate AS, (D) RL-BAV without AS, (E) RL-BAV with moderate AS, (F) RN-BAV without AS and (G) RN-BAV with moderate AS. 2D indicates 2-dimensional; 3D, 3-dimensional; 4D, 4-dimensional; AAo, ascending aorta; AS, aortic stenosis; AV, aortic valve; BAV, bicuspid aortic valve; LV, left ventricle; MRI, magnetic resonance imaging; RL-BAV, right and left coronary leaflet fusion BAV; RN-BAV, right and noncoronary leaflet fusion BAV; RPA, right pulmonary artery; SSFP, steady state free precession; TAV-TAA, tricuspid aortic valve with aortic dilation. Arrows indicate high-velocity outflow jets in RL-BAV and RN-BAV without AS.

distal AAo, compared with controls (WSS was increased by 30% at the outer distal AAo only; $P<0.001$).

3D WSS in Patients With Mild AS

The presence of mild stenosis altered WSS distributions for all TAV and BAV patient groups. As shown in Figure 3E and Table 2, aortic WSS was elevated for the TAV-TAA group on the outer proximal aorta by 57% compared with controls. Elevated WSS was also found on the proximal and distal outer curvature of the aorta and the inner proximal aorta for RL-BAV compared with controls. Compared with TAV-TAA, elevated WSS was found on the outer distal AAo and the inner proximal AAo. RN-BAV demonstrated elevated WSS on the proximal

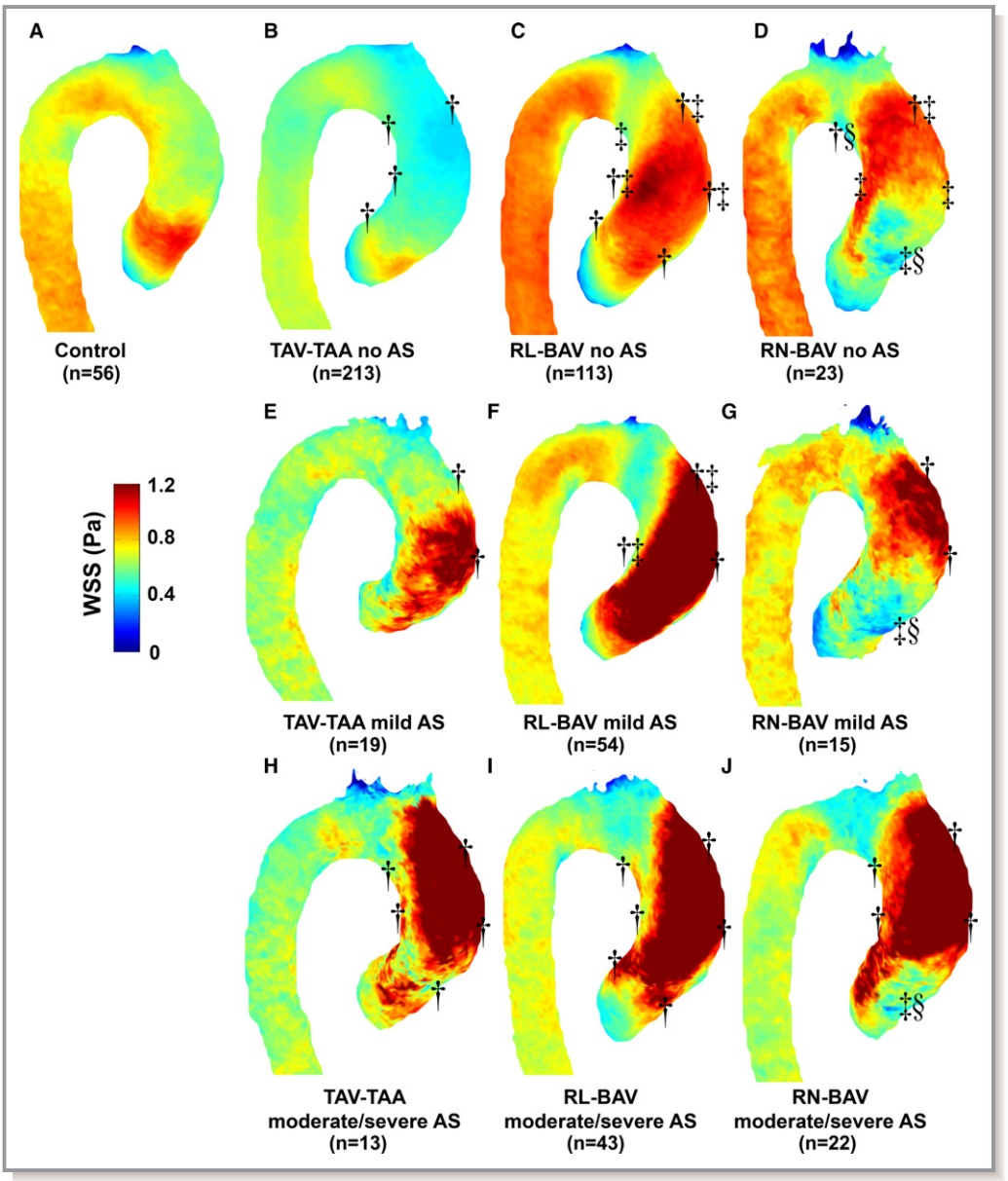

Figure 3. Atlases of WSS for (A) controls, (B) TAV-TAA without AS, (C) RL-BAV without AS, (D) RN-BAV without AS, (E through G) the corresponding patients with mild AS, and (H through J) the corresponding patients with moderate/severe AS. Significant differences in WSS in the 6 regions of interest are marked by a dagger ("†") for comparisons to controls, a double dagger ("‡") for "within AS group" comparisons to TAV-TAA, and a section mark ("§") for "within AS group" comparisons to RL-BAV (analysis adjusted for age and sex). Note: "within AS group" refers to those atlases with a similar degree of AS (eg, only atlases in the same rows were compared to one another). AS indicates aortic stenosis; BAV, bicuspid aortic valve; RL-BAV, right and left coronary leaflet fusion BAV; RN-BAV, right and noncoronary leaflet fusion BAV; TAV-TAA, tricuspid aortic valve with aortic dilation; WSS, wall shear stress.

Table 2. Median WSS and Interquartile Ranges for Controls vs TAV-TAA, RL-BAV, and RN-BAV Without AS

Regional WSS (Pa)	Controls	TAV-TAA	RL-BAV	RN-BAV
No AS				
Inner root AAo	0.80 (0.54–1.06)	0.61 (0.36–0.88)*	0.67 (0.40–0.94)*	0.68 (0.43–0.97)
Outer root AAo	0.70 (0.44–0.93)	0.69 (0.39–0.94)	0.82 (0.55–1.03)*	0.62 (0.32–0.88)†,‡
Inner proximal AAo	0.65 (0.44–0.85)	0.44 (0.28–0.64)*	0.78 (0.50–1.06)*,†	0.73 (0.42–1.08)†
Outer proximal AAo	0.56 (0.40–0.71)	0.44 (0.28–0.65)	0.73 (0.44–1.01)*,†	0.62 (0.42–0.87)†
Inner distal AAo	0.65 (0.51–0.81)	0.47 (0.33–0.63)*	0.71 (0.51–0.96)†	0.57 (0.35–0.94)*,‡
Outer distal AAo	0.61 (0.48–0.75)	0.41 (0.30–0.54)*	0.82 (0.57–1.15)*,†	0.79 (0.55–1.06)*,†
Mild AS				
Inner root AAo	0.80 (0.54–1.06)	0.68 (0.40–1.07)	0.93 (0.56–1.34)	0.74 (0.45–1.05)
Outer root AAo	0.70 (0.44–0.93)	0.75 (0.41–1.23)	0.99 (0.58–1.43)	0.53 (0.32–0.86)†,‡
Inner proximal AAo	0.65 (0.44–0.85)	0.51 (0.29–0.78)	0.80 (0.52–1.24)*,†	0.75 (0.47–1.09)
Outer proximal AAo	0.56 (0.40–0.71)	0.88 (0.48–1.36)*	0.95 (0.49–1.47)*	0.70 (0.47–1.02)*
Inner distal AAo	0.65 (0.51–0.81)	0.52 (0.31–0.76)	0.65 (0.44–0.93)	0.58 (0.40–0.88)
Outer distal AAo	0.61 (0.48–0.75)	0.60 (0.38–0.93)*	1.19 (0.74–1.55)*,†	0.95 (0.62–1.31)*
Moderate and severe AS				
Inner root AAo	0.80 (0.54–1.06)	0.90 (0.54–1.33)	0.93 (0.63–1.44)*	0.95 (0.51–1.52)
Outer root AAo	0.70 (0.44–0.93)	0.81 (0.51–1.19)*	0.88 (0.56–1.34)*	0.64 (0.36–1.00)†,‡
Inner proximal AAo	0.65 (0.44–0.85)	0.93 (0.59–1.30)*	0.90 (0.62–1.37)*	0.98 (0.60–1.65)*
Outer proximal AAo	0.56 (0.40–0.71)	1.08 (0.69–1.55)*	0.97 (0.57–1.63)*	0.96 (0.63–1.41)*
Inner distal AAo	0.65 (0.51–0.81)	0.82 (0.49–1.27)*	0.89 (0.57–1.27)*	0.87 (0.54–1.32)*
Outer distal AAo	0.61 (0.48–0.75)	1.53 (1.05–1.95)*	1.69 (1.24–2.08)*	1.44 (0.98–1.87)*

AAo indicates ascending aorta; AS, aortic stenosis; BAV, bicuspid aortic valve; RL-BAV, right and left coronary leaflet fusion BAV; RN-BAV, right and non-coronary leaflet fusion BAV; TAV-TAA, tricuspid aortic valve with aortic dilation; WSS, wall shear stress.
*Significantly different vs controls.
†Significantly different vs TAV-TAA.
‡Significantly different vs RL-BAV (adjusted for age and sex).

and distal outer AAo, whereas decreased WSS was found on the outer root compared with controls. Compared with TAV-TAA and RL-BAV, RN-BAV demonstrated decreased WSS on the outer root. Notably, TAV-TAA patients with mild AS demonstrated an inverse WSS pattern (elevated WSS) compared with the no AS group (reduced WSS) and controls.

3D WSS in Patients With Moderate or Severe AS

The presence of moderate and severe AS further altered WSS distributions for all TAV and BAV patient groups. As shown in Figure 3H through 3J and Table 2, aortic WSS was elevated for all patient groups with moderate or severe AS compared with controls in all AAo regions except for the inner aortic root for TAV-TAA and RN-BAV and the outer root for RN-BAV. As opposed to WSS findings in patients without AS, differences between BAV cusp fusion patterns (RL-BAV versus RN-BAV) and between valve phenotypes (BAV versus TAV-TAA) in the presence of moderate or severe AS were no longer apparent. There were no significant differences between TAV-TAA, RL-BAV, and RN-BAV with moderate or severe AS in any of the 6 regions, except for significant lower WSS for RN-BAV compared with TAV-TAA and RL-BAV on the outer AAo (Figure 3J, Table 2).

3D WSS Variability Across Cohorts

The variability (IQR) of systolic 3D WSS between patients in each cohort (RL-BAV, RN-BAV, TAV-TAA, and controls) and those with no AS, mild AS, and moderate-to-severe AS is illustrated in Figure 4 and summarized in Table 3. Compared with patients with no AS (Figure 4, top row), WSS variability in patients with mild AS (Figure 4, middle row) and patients with moderate or severe AS (Figure 4, lower row) was considerably increased throughout the entire aorta (by 20–178% for TAV-TAA, 37–111% for RL-BAV, and 14–109% for RN-BAV for no AS compared with moderate or severe AS). These findings indicate that WSS patterns were similar across subject groups

without AS whereas the presence of AS introduced increased variability of WSS patterns between individual patients.

Discussion

The findings of this cross-sectional study reinforce the notion that patients at risk of aortopathy have distinctly altered cohort-specific 3D WSS patterns in the AAo compared with healthy controls. In the largest 4D flow MRI study to date, we have confirmed that: (1) BAV is associated with elevated aortic WSS even in the absence of AS, and BAV cusp fusion morphology significantly impacts the eccentric distribution of 3D WSS in the AAo; (2) 3D WSS in TAV-TAA patients without AS is significantly reduced compared with controls and homogenously distributed throughout the ascending aorta; and (3) in patients with any degree of AS, the variability and

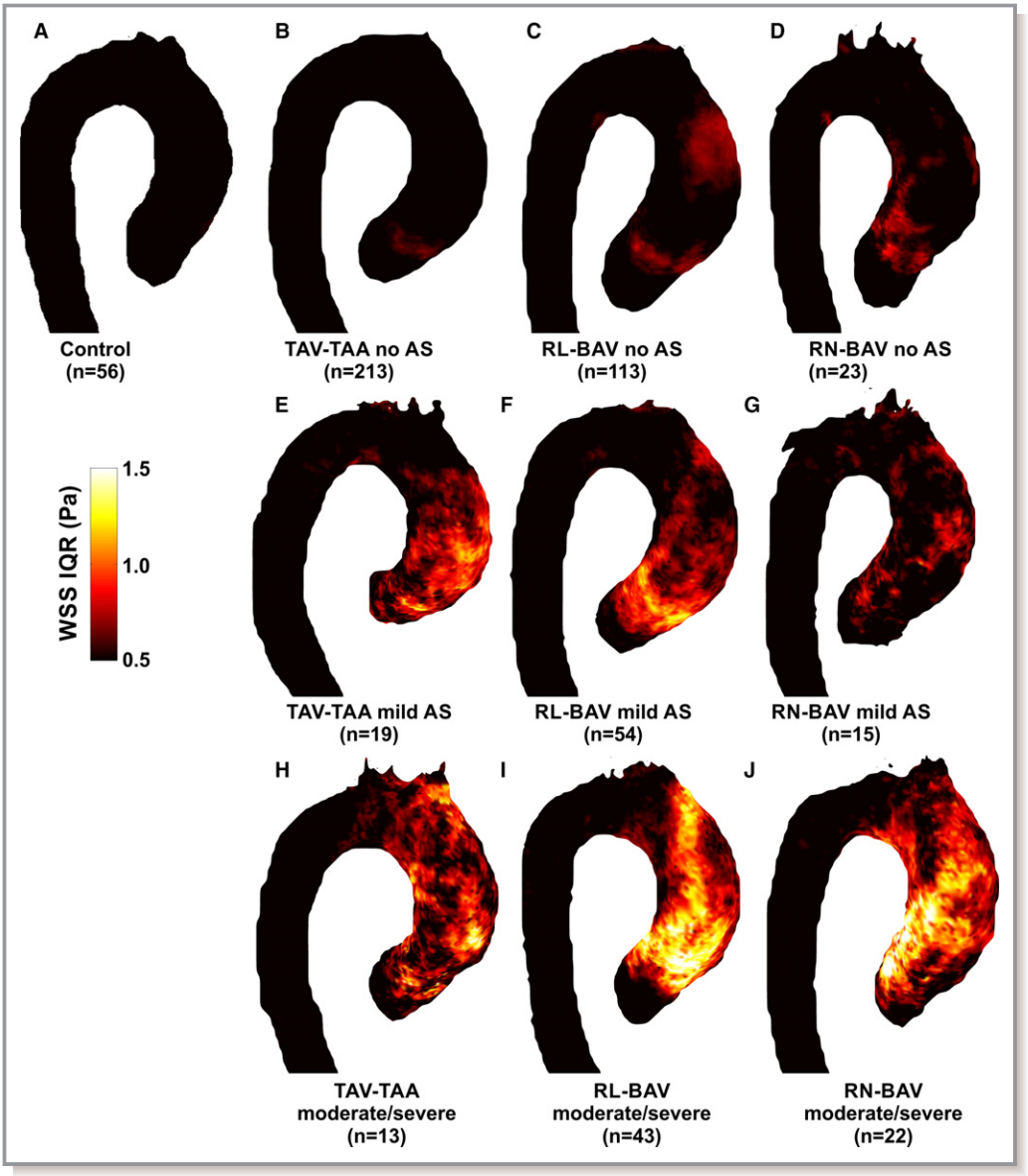

Figure 4. Atlases of WSS interquartile range (IQR) for (A) controls, (B) TAV-TAA without AS, (C) RL-BAV without AS, (D) RN-BAV without AS, (E through G) the corresponding patients with mild AS, and (H through J) the corresponding patients with moderate/severe AS. IQR is expressed as the range between the 75% and 25% quartile of WSS magnitude for all subjects in a given cohort. This represents the regional variability of WSS experienced across the subjects in each group. Controls and patients with no AS (top row) had relatively low WSS variability in the thoracic aorta with mildly elevated WSS IQR in the ascending aorta of BAV patients. In contrast, WSS variability was markedly elevated in the ascending aorta of most AS patient groups (RL-BAV, RN-BAV, TAV, and dilated aorta). Color coding=intersubject IQR of WSS magnitude. AS indicates aortic stenosis; BAV, bicuspid aortic valve; RL-BAV, right and left coronary leaflet fusion BAV; RN-BAV, right and noncoronary leaflet fusion BAV; TAV-TAA, tricuspid aortic valve with aortic dilation; WSS, wall shear stress.

Table 3. IQRs (Expressed as the Difference Between 75% and 25%) of the Cohort-Averaged WSS Maps

WSS IQR Range (Pa)	Controls	No AS			Mild AS			Moderate and Severe AS		
		TAV-TAA	RL-BAV	RN-BAV	TAV-TAA	RL-BAV	RN-BAV	TAV-TAA	RL-BAV	RN-BAV
Inner root AAo	0.41	0.46	0.44	0.50	0.57	0.74	0.53	0.69	0.93	0.99
Outer root AAo	0.41	0.50	0.47	0.45	0.72	0.78	0.39	0.60	0.89	0.56
Inner proximal AAo	0.33	0.32	0.43	0.56	0.39	0.48	0.53	0.63	0.59	0.98
Outer proximal AAo	0.28	0.35	0.44	0.38	0.74	0.61	0.49	0.62	0.66	0.64
Inner distal AAo	0.27	0.28	0.40	0.35	0.41	0.41	0.33	0.66	0.64	0.73
Outer distal AAo	0.26	0.23	0.54	0.42	0.47	0.59	0.52	0.64	0.69	0.72

AAo indicates ascending aorta; AS, aortic stenosis; BAV, bicuspid aortic valve; IQR, interquartile range; RL-BAV, right and left coronary leaflet fusion BAV; RN-BAV, right and noncoronary leaflet fusion BAV; TAV-TAA, tricuspid aortic valve with aortic dilation; WSS, wall shear stress.

magnitude of 3D WSS patterns is significantly higher compared with groups without AS, and WSS differences between valve phenotypes (RL-BAV, RN-BAV, TAV) are no longer apparent.

Bicuspid Aortic Valve Disease

Even in the absence of aortic valve stenosis, the congenitally abnormal BAV is thought to introduce abnormal systolic outflow patterns impinging on the aortic wall, thereby creating specific regions of elevated WSS. Moreover, compared to the normal aortic valve, blood flow through the BAV is altered as a function of the cusp fusion phenotype, the most common of which are the right-left or right-noncoronary leaflet fusion patterns. This flow physiology was confirmed by our findings, which exhibit eccentric and higher WSS on the entire AAo for RL-BAV patients, whereas RN-BAV patients demonstrated more-focal WSS elevation concentrated at the outer distal AAo. The low WSS variability (IQR) across a large cohort of nonstenotic BAV patients (n=113 RL-BAV; n=23 RN-BAV) suggests that BAV-mediated changes in WSS are consistent across nonstenotic patients and associated with the cusp fusion phenotype. Interestingly, these regions of increased WSS corresponded with known differences in aortopathy expression for RL-BAV and RN-BAV: Dilatation of the tubular AAo accompanied by aortic-root dilatation has been associated with RL-BAV, whereas more-distal dilatation of the tubular AAo extending to the proximal arch with sparing of the aortic root has been associated with RN-BAV.[27] These findings therefore support the notion that increased WSS may influence outward vessel remodeling in the presence of BAV aortopathy.[28] It should be noted, however, that in this cross-sectional study, correlation of WSS in the chosen regions of interest (shown in Figure 1) did not exhibit statistically significant associations to diameter. Longitudinal studies (on the order of decades) and additional methodological developments taking into account specific "abnormal" WSS regions are needed to further investigate this hypothesis.

Other studies have implicated WSS and its potential role in the aortic dilatation process for BAV patients. Barker et al and Hope et al were the first to link eccentric flow patterns in BAV disease with WSS, as measured with 2D flow MRI and 4D flow MRI, respectively.[29,30] Similar to our study, maximum systolic WSS was found in different aortic regions for RL-BAV and RN-BAV. These findings were confirmed by Bissel et al and Mahadevia et al in larger cohorts (142 and 75 subjects, respectively).[7,31] However, an important shortcoming of past studies is related to the use of manually positioned 2D analysis planes for the calculation of WSS, which resulted in limited coverage of the complex and asymmetric WSS distribution in the aorta. In contrast, the 3D WSS calculation and atlas approach used in this study allowed for a comprehensive, yet concise, visualization and quantification of WSS behavior along the entire surface of the aorta.

Aortic Dilatation in Patients With TAV

Aortic dilatation in the setting of a normal functioning TAV resulted in a reduced and more-homogenous distribution of WSS. Other studies confirm our findings[10,11] and align with the idea that WSS should be reduced in the presence of an enlarged vessel (holding stroke volume constant: mean velocity and thus velocity gradients will be reduced, which, in turn, will reduce WSS).[32] The presence of vortex and supraphysiological helical flow has shown to be significantly increased in the setting of the dilated ascending aorta and an increase in ascending aortic diameter is significantly correlated with the presence of aberrant flow (elevated helix and vortex formation).[33] These observed blood flow patterns were associated with changes in regional peak systolic WSS in the AAo and proximal aortic arch. Significant reductions in regional peak systolic WSS were more pronounced along the right outer aortic wall. Moreover, increased vessel

diameter was inversely correlated to peak systolic WSS, indicating a relationship between dilatation and reduction in WSS in patients with vessel dilation but otherwise normal physiology. We postulate that the WSS relationship to size in this TAV group is not pathological, rather a manifestation of increasing vessel caliber outside of the influence of WSS. For example, in the very simplified situation of a straight rigid pipe with steady Poiseuille flow (ie, a fully developed parabolic flow profile where viscous effects dominate over inertial effects), the relationship of WSS to flow and diameter is WSS—[viscosity×flow/diameter^3]. If viscosity and flow are held constant, an increase in diameter will decrease WSS by an inverse cubic function. A similar behavior has been found in the pulmonary arteries of pulmonary arterial hypertension patients.[32]

Because of referral patterns and natural history (onset of dilatation later in life for TAV patients), BAV and TAV cohorts had differences in age. WSS decreases with age in healthy controls attributed to natural aorta growth.[34] However, the WSS values found in the TAV-TAA group here (0.51 Pa averaged over the entire AAo) are lower than that reported for an age-matched control group of 51- to 60-year-olds reported in a previous study (0.59 Pa); thus, we feel the impact of size contributed beyond age effects.[34] The inverse size/WSS relationship does not hold for the larger vessel diameters found in the BAV patients, given that the malformed valve acts as a flow trip (ie, a geometrical obstruction), which causes eccentric flow in the BAV patients and thereby elevates the regional WSS in the vicinity.

Impact of AS

A previous study from our group found that AS did not elevate WSS in a small pilot cohort of BAV patients (of n=15, only 8 had AS).[6] Contrary to the previous findings, this study found marked, significant increases of aortic 3D WSS in the presence of AS for both TAV-TAA and BAV groups (Figure 3; Table 2). We suspect that the previous study did not have sufficient power to detect differences of regional WSS between the AS groups, especially given the new data measuring interpatient WSS variability (see IQR of the AS groups in Figure 4). Also notable is that the regional differences of WSS distribution for the BAV and TAV-TAA groups with no AS were no longer apparent in the presence of moderate or severe AS (eg, eccentric high WSS for BAV versus homogenous low WSS for aortic dilatation and TAV-TAA). Finally, the increased variability in 3D WSS patterns for patients with AS indicates the increased variability of the transvalvular outflow and resulting 3D WSS patterns. We postulate that lesions such as calcifications are less predictable than the cusp fusion patterns in their effect on transvalvular flow, thus resulting in a larger interpatient IQR in the AS populations. These findings also imply that AS overrides the previously described flow patterns associated with BAV and/or TAV-TAA and dominates ascending aortic hemodynamics irrespective of valve phenotype.

Similar to our findings, studies have shown that the presence of aortic valve disease has a very different effect on aortic hemodynamics as compared to aortic dilatation or aneurysm alone.[12] Findings demonstrate that aortic dilatation with an otherwise normal aortic valve (TAV) generally leads to deranged (helical) slow flow with significantly lower WSS in the ascending aorta.[10] In contrast, BAV or AS will result in significantly elevated flow velocities, localized outflow jet patterns, and eccentrically elevated WSS.[6,7] These observations indicate that aortic valve disease and aortic dilatation represent different manifestation of aortic pathologies that may lead to similar patient outcome (aneurysm, dissection), but are associated with substantially differing hemodynamics and WSS. If changes in aortic hemodynamics are considered a contributing factor for aortopathy progression, it may be attributed to different underlying pathophysiological mechanisms for AS (outflow jets and eccentrically elevated WSS) and aortic dilatation (slow helix flow and low WSS). In addition, consideration must be given that hemodynamics may exacerbate pathology in a genetically susceptible aorta and thereby hemodynamic stimulus in some groups (such as BAV subjects) may be more important than others.

Thus, the significance of the observed changes in aortic hemodynamics continues to be a subject of ongoing debate (Are flow alterations the consequence of aortic disease or do they play an active role in development of aortopathy?). There is growing evidence that flow changes may play an active role in the development of aortopathy such as dilatation, aneurysm, or dissection. For example, WSS is known to alter function and gene expression of the endothelial cells lining the initial vessel wall and has been implicated in aortic wall remodeling in previous studies.[35] Recent work by Guzzardi et al has shown that regions of increased WSS, measured by 4D flow MRI in BAV patients before aortic valve repair, corresponded with extracellular matrix dysregulation and elastic fiber degeneration in resected tissue samples from the same patients.[8] Tsamis et al found that BAV patients exhibit asymmetric dilatation of the greater curvature of the aorta, compared to symmetric dilatation in TAV patients, concomitant with different elastin and collagen fiber orientation between the types of valves.[36] Additionally, Girdauskas et al recently determined that there was no difference in correlation patterns between functional aortic root parameters and expression of aortopathy between BAV and TAV patients with aortic dilatation and AS.[9] The findings of our study indicate that these apparent contradictions may be brought about by the presence of AS, which can significantly alter and dominate aortic 3D WSS patterns irrespective of valve type.

It is still unclear whether genetic predisposition leads to aortopathy or whether the altered BAV morphology creates local areas of disease within the aortic wall related to abnormal blood flow from the valve. It is possible that it is a combination of both, but a focus on the genetic axiom for BAV aortopathy has encouraged aggressive surgical management strategies with respect to the timing and extent of aortic resection (early and wide surgical resection). Additionally, historical research on the hemodynamic hypothesis for BAV-related aortopathy has focused on degree of AS or aortic regurgitation. These measures of valve function are important to control for when studying aortopathy; however, this study shows that these metrics alone may not reflect the burden on the aortic wall attributed to a functional, yet malformed valve. This study illustrates a method to study the possible role of near wall hemodynamics and the development of aortopathy in a large cohort of patients.

Study Limitations

The cause of AS was not recorded in this study (such as rheumatic heart disease, etc); future studies should take this into consideration. Aortic regurgitation is an additional risk factor for aortopathy[1]; however, it is difficult to quantify diastolic WSS attributed to low signal-to-noise ratio with 4D flow MRI and the need for a time resolved segmentation to capture aortic root motion. Given the results from previous studies showing the greatest flow differences between patient groups occur at systole,[29] we chose to focus on systolic WSS. Therefore, an important, yet separate, patient group with regurgitation remains to be examined. An additional challenge associated with WSS determination is aortic root motion. As a result, we used a recently described method, which does not require a time-resolved segmentation and has been found robust in the computation of WSS from a systolic phase-contrast magnetic resonance angiography geometry and the associated systolic velocity field.[14] However, regions of slow and recirculating flow can be difficult to capture with the phase-contrast magnetic resonance angiography approach. This has not been shown to affect the ability to capture the root geometry downstream from the sinotubular junction; however, some error may be present for WSS values measured in the region of the sinus of Valsalva.[26] 4D flow MRI is lengthy (≈10 minutes) and involves time-consuming data analysis; however, improvements in software tools, sequence implementation, and compressed sensing methods have positioned this technique to be clinically viable in the near future. We used both 1.5 and 3 Tesla MRI exams for this study, it should be noted that previous studies investigated the effect of field strength on image quality and the ability to measure WSS and no differences were found.[37] Observer variability and test-retest were not assessed in this study because previous studies have demonstrated excellent inter-observer variability and test-retest reproducibility of the 3D WSS method and 3D WSS atlas concept.[14]

Conclusion

AS significantly alters aortic hemodynamics and 3D WSS independent of aortic valve phenotype and over-rides previously described flow patterns associated with BAV and TAV with aortic dilatation. Severity of AS must be considered when investigating valve-mediated aortopathy.

Sources of Funding

Research reported in this publication was supported by the National Heart, Lung, and Blood Institute of the NIH under Award Nos. K25HL119608, R01HL115828, and R01HL133504. The content is solely the responsibility of the authors and does not necessarily represent the official views of the NIH. Additional support from the Martha and Richard Melman Family Bicuspid Aortic Valve Program, Bluhm Cardiovascular Institute, Northwestern Medicine.

Acknowledgments

The authors thank Alexander Powell and the Northwestern University's Center for Translational Imaging for aid in data collection, collation, and organization.

Disclosures

None.

References

1. Roberts WC, Vowels TJ, Ko JM, Filardo G, Hebeler RF Jr, Henry AC, Matter GJ, Hamman BL. Comparison of the structure of the aortic valve and ascending aorta in adults having aortic valve replacement for aortic stenosis versus for pure aortic regurgitation and resection of the ascending aorta for aneurysm. *Circulation*. 2011;123:896–903.
2. Verma S, Siu SC. Aortic dilatation in patients with bicuspid aortic valve. *N Engl J Med*. 2014;370:1920–1929.
3. Fedak PWM, Verma S, David TE, Leask RL, Weisel RD, Butany J. Clinical and pathophysiological implications of a bicuspid aortic valve. *Circulation*. 2002;106:900–904.
4. Michelena HI, Khanna AD, Mahoney D, Margaryan E, Topilsky Y, Suri RM, Eidem B, Edwards WD, Sundt TM III, Enriquez-Sarano M. Incidence of aortic complications in patients with bicuspid aortic valves. *JAMA*. 2011;306:1104–1112.
5. Michelena HI, Prakash SK, Della Corte A, Bissell MM, Anavekar N, Mathieu P, Bossé Y, Limongelli G, Bossone E, Benson DW, Lancellotti P, Isselbacher EM, Enriquez-Sarano M, Sundt TM III, Pibarot P, Evangelista A, Milewicz DM, Body SC; BAVCon Investigators. Bicuspid aortic valve: identifying knowledge gaps and rising to the challenge from the International Bicuspid Aortic Valve Consortium (BAVCon). *Circulation*. 2014;129:2691–2704.
6. Barker AJ, Markl M, Burk J, Lorenz R, Bock J, Bauer S, Schulz-Menger J, von Knobelsdorff-Brenkenhoff F. Bicuspid aortic valve is associated with altered wall shear stress in the ascending aorta. *Circ Cardiovasc Imaging*. 2012;5:457–466.

7. Mahadevia R, Barker AJ, Schnell S, Entezari P, Kansal P, Fedak PW, Malaisrie SC, McCarthy P, Collins J, Carr J, Markl M. Bicuspid aortic cusp fusion morphology alters aortic three-dimensional outflow patterns, wall shear stress, and expression of aortopathy. *Circulation*. 2014;129:673–682.
8. Guzzardi DG, Barker AJ, van Ooij P, Malaisrie SC, Puthumana JJ, Belke DD, Mewhort HE, Svystonyuk DA, Kang S, Verma S, Collins J, Carr J, Bonow RO, Markl M, Thomas JD, McCarthy PM, Fedak PW. Valve-related hemodynamics mediate human bicuspid aortopathy: insights from wall shear stress mapping. *J Am Coll Cardiol*. 2015;66:892–900.
9. Girdauskas E, Rouman M, Disha K, Scholle T, Fey B, Theis B, Petersen I, Borger MA, Kuntze T. Correlation between systolic transvalvular flow and proximal aortic wall changes in bicuspid aortic valve stenosis. *Eur J Cardiothorac Surg*. 2014;46:234–239; discussion, 239.
10. Burk J, Blanke P, Stankovic Z, Barker A, Russe M, Geiger J, Frydrychowicz A, Langer M, Markl M. Evaluation of 3D blood flow patterns and wall shear stress in the normal and dilated thoracic aorta using flow-sensitive 4D CMR. *J Cardiovasc Magn Reson*. 2012;14:84.
11. Bieging ET, Frydrychowicz A, Wentland A, Landgraf BR, Johnson KM, Wieben O, Francois CJ. In vivo three-dimensional MR wall shear stress estimation in ascending aortic dilatation. *J Magn Reson Imaging*. 2011;33:589–597.
12. van Ooij P, Potters WV, Nederveen AJ, Allen BD, Collins J, Carr J, Malaisrie SC, Markl M, Barker AJ. A methodology to detect abnormal relative wall shear stress on the full surface of the thoracic aorta using four-dimensional flow MRI. *Magn Reson Med*. 2015;73:1216–1227.
13. van Ooij P, Potters WV, Collins J, Carr M, Carr J, Malaisrie SC, Fedak PW, McCarthy PM, Markl M, Barker AJ. Characterization of abnormal wall shear stress using 4D flow MRI in human bicuspid aortopathy. *Ann Biomed Eng*. 2015;43:1385–1397.
14. van Ooij P, Powell AL, Potters WV, Carr JC, Markl M, Barker AA. Reproducibility and interobserver variability of systolic blood flow velocity and 3D wall shear stress derived from 4D flow MRI in the healthy aorta. *J Magn Reson Imaging*. 2016;43:236–248.
15. Malaisrie SC, Carr J, Mikati I, Rigolin V, Yip BK, Lapin B, McCarthy PM. Cardiac magnetic resonance imaging is more diagnostic than 2-dimensional echocardiography in determining the presence of bicuspid aortic valve. *J Thorac Cardiovasc Surg*. 2012;144:370–376.
16. Trinh B, Dubin I, Rahman O, Botelho MPF, Naro N, Carr JC, Collins JD, Barker AJ. Aortic volumetry at contrast-enhanced magnetic resonance angiography. *Invest Radiol*. 2017;52:216–222.
17. Dyverfeldt P, Bissell M, Barker AJ, Bolger AF, Carlhall CJ, Ebbers T, Francios CJ, Frydrychowicz A, Geiger J, Giese D, Hope MD, Kilner PJ, Kozerke S, Myerson S, Neubauer S, Wieben O, Markl M. 4D flow cardiovascular magnetic resonance consensus statement. *J Cardiovasc Magn Reson*. 2015;17:72.
18. Sievers HH, Schmidtke C. A classification system for the bicuspid aortic valve from 304 surgical specimens. *J Thorac Cardiovasc Surg*. 2007;133:1226–1233.
19. Hiratzka LF, Bakris GL, Beckman JA, Bersin RM, Carr VF, Casey DE Jr, Eagle KA, Hermann LK, Isselbacher EM, Kazerooni EA, Kouchoukos NT, Lytle BW, Milewicz DM, Reich DL, Sen S, Shinn JA, Svensson LG, Williams DM; American College of Cardiology Foundation/American Heart Association Task Force on Practice Guidelines; American Association for Thoracic Surgery; American College of Radiology; American Stroke Association; Society of Cardiovascular Anesthesiologists; Society for Cardiovascular Angiography and Interventions; Society of Interventional Radiology; Society of Thoracic Surgeons; Society for Vascular Medicine. 2010 ACCF/AHA/AATS/ACR/ASA/SCA/SCAI/SIR/STS/SVM guidelines for the diagnosis and management of patients with thoracic aortic disease. *Circulation*. 2010;121:e266–e369.
20. Bock J, Kreher BW, Hennig J, Markl M. Optimized pre-processing of time-resolved 2D and 3D phase contrast MRI data. Proceedings of the 15th Scientific Meeting of the International Society of Magnetic Resonance in Medicine. Wiley 2007:3138. Berlin, Germany.
21. Bock J, Frydrychowicz A, Stalder AF, Bley TA, Burkhardt H, Hennig J, Markl M. 4D phase contrast MRI at 3 T: effect of standard and blood-pool contrast agents on SNR, PC-MRA, and blood flow visualization. *Magn Reson Med*. 2010;63:330–338.
22. Rose MJ, Jarvis K, Chowdhary V, Barker AJ, Allen BD, Robinson JD, Markl M, Rigsby CK, Schnell S. Efficient method for volumetric assessment of peak blood flow velocity using 4D flow MRI. *J Magn Reson Imaging*. 2016;44:1673–1682.
23. Nishimura RA, Otto CM, Bonow RO, Carabello BA, Erwin JP III, Guyton RA, O'Gara PT, Ruiz CE, Skubas NJ, Sorajja P, Sundt TM III, Thomas JD; ACC/AHA Task Force Members. 2014 AHA/ACC guideline for the management of patients with valvular heart disease: a report of the American College of Cardiology/American Heart Association Task Force on Practice Guidelines. *Circulation*. 2014;129:e521–e643.
24. Cawley PJ, Maki JH, Otto CM. Cardiovascular magnetic resonance imaging for valvular heart disease: technique and validation. *Circulation*. 2009;119:468–478.
25. Potters WV, van Ooij P, Marquering H, van Bavel E, Nederveen AJ. Volumetric arterial wall shear stress calculation based on cine phase contrast MRI. *J Magn Reson Imaging*. 2015;41:505–516.
26. Garcia J, Barker AJ, Murphy I, Jarvis K, Schnell S, Collins JD, Carr JC, Malaisrie SC, Markl M. Four-dimensional flow magnetic resonance imaging-based characterization of aortic morphometry and haemodynamics: impact of age, aortic diameter, and valve morphology. *Eur Heart J Cardiovasc Imaging*. 2016;17:877–884.
27. Kang JW, Song HG, Yang DH, Baek S, Kim DH, Song JM, Kang DH, Lim TH, Song JK. Association between bicuspid aortic valve phenotype and patterns of valvular dysfunction and bicuspid aortopathy comprehensive evaluation using MDCT and echocardiography. *JACC Cardiovasc Imaging*. 2013;6:150–161.
28. Dolan JM, Kolega J, Meng H. High wall shear stress and spatial gradients in vascular pathology: a review. *Ann Biomed Eng*. 2013;41:1411–1427.
29. Barker AJ, Lanning C, Shandas R. Quantification of hemodynamic wall shear stress in patients with bicuspid aortic valve using phase-contrast MRI. *Ann Biomed Eng*. 2010;38:788–800.
30. Hope MD, Hope TA, Meadows AK, Ordovas KG, Urbania TH, Alley MT, Higgins CB. Bicuspid aortic valve: four-dimensional MR evaluation of ascending aortic systolic flow patterns. *Radiology*. 2010;255:53–61.
31. Bissell MM, Hess AT, Biasiolli L, Glaze SJ, Loudon M, Pitcher A, Davis A, Prendergast B, Markl M, Barker AJ, Neubauer S, Myerson SG. Aortic dilation in bicuspid aortic valve disease: flow pattern is a major contributor and differs with valve fusion type. *Circ Cardiovasc Imaging*. 2013;6:499–507.
32. Truong U, Fonseca B, Dunning J, Burgett S, Lanning C, Ivy DD, Shandas R, Hunter K, Barker AJ. Wall shear stress measured by phase contrast cardiovascular magnetic resonance in children and adolescents with pulmonary arterial hypertension. *J Cardiovasc Magn Reson*. 2013;15:81.
33. Frydrychowicz A, Berger A, Munoz Del Rio A, Russe MF, Bock J, Harloff A, Markl M. Interdependencies of aortic arch secondary flow patterns, geometry, and age analysed by 4-dimensional phase contrast magnetic resonance imaging at 3 Tesla. *Eur Radiol*. 2012;22:1122–1130.
34. van Ooij P, Garcia J, Potters WV, Malaisrie SC, Collins JD, Carr JC, Markl M, Barker AJ. Age-related changes in aortic 3D blood flow velocities and wall shear stress: implications for the identification of altered hemodynamics in patients with aortic valve disease. *J Magn Reson Imaging*. 2016;43:1239–1249.
35. Lehoux S, Tedgui A. Cellular mechanics and gene expression in blood vessels. *J Biomech*. 2003;36:631–643.
36. Tsamis A, Phillippi JA, Koch RG, Chan PG, Krawiec JT, D'Amore A, Watkins SC, Wagner WR, Vorp DA, Gleason TG. Extracellular matrix fiber microarchitecture is region-specific in bicuspid aortic valve-associated ascending aortopathy. *J Thorac Cardiovasc Surg*. 2016;151:1718–1728.e5.
37. Strecker C, Harloff A, Wallis W, Markl M. Flow-sensitive 4D MRI of the thoracic aorta: comparison of image quality, quantitative flow, and wall parameters at 1.5 T and 3 T. *J Magn Reson Imaging*. 2012;36:1097–1103.